

## RESEARCH ARTICLE

# Shotgun proteome analysis of *Bordetella pertussis* reveals a distinct influence of iron availability on the bacterial metabolism, virulence, and defense response

Jimena Alvarez Hayes<sup>1\*</sup>, Yanina Lamberti<sup>1\*</sup>, Kristin Surmann<sup>2</sup>, Frank Schmidt<sup>2,3</sup>, Uwe Völker<sup>2</sup> and Maria Eugenia Rodriguez<sup>1</sup>

<sup>1</sup> CINDEFI (UNLP CONICET La Plata), Facultad de Ciencias Exactas, Universidad Nacional de La Plata, La Plata, Argentina

<sup>2</sup> Interfaculty Institute for Genetics and Functional Genomics, University Medicine Greifswald, Greifswald, Germany

<sup>3</sup> ZIK-FunGene Junior Research Group Applied Proteomics, University Medicine Greifswald, Greifswald, Germany

One of the mechanisms involved in host immunity is the limitation of iron accessibility to pathogens, which in turn provokes the corresponding physiological adaptation of pathogens. This study reports a gel-free nanoLC-MS/MS-based comparative proteome analysis of *Bordetella pertussis* grown under iron-excess and iron-depleted conditions. Out of the 926 proteins covered 98 displayed a shift in their abundance in response to low iron availability. Forty-seven of them were found to be increased in level while 58 were found with decreased protein levels under iron starvation. In addition to proteins previously reported to be influenced by iron in *B. pertussis*, we observed changes in metabolic proteins involved in fatty acid utilization and poly-hydroxybutyrate production. Additionally, many bacterial virulence factors regulated by the BvgAS two-component system were found at decreased levels in response to iron limitation. These results, together with the increased production of proteins potentially involved in oxidative stress resistance, seem to indicate that iron starvation provokes changes in *B. pertussis* phenotype that might shape host–pathogen interaction.

**Keywords:**

*Bordetella pertussis* / Fatty acid degradation / Iron starvation / Microbiology / Oxidative stress response / Virulence factors expression



Additional supporting information may be found in the online version of this article at the publisher's web-site

## 1 Introduction

Iron is a vital nutrient for bacteria. The presence of glycoproteins such as transferrin and lactoferrin, or hemoproteins like hemoglobin determines a concentration of free iron in the human body too low to support bacterial growth. Pathogens have evolved to acquire iron through different mechanisms such as specific receptors for direct acquisition of iron from transferrin, lactoferrin, or hemoglobin, or through the production

and utilization of low-molecular-weight iron chelators named siderophores.

*Bordetella pertussis*, the causative agent of pertussis or whooping cough, is a strictly human-adapted pathogen. *Bordetella pertussis* obtains iron from the host by means of production and use of the siderophore alcaligin [1] or the use of the xenosiderophore enterobactin [2]. This bacterium is also capable of using hemin as iron source [3]. In vivo studies have shown that all of these systems are expressed during infection [4], confirming that *B. pertussis* is iron-starved inside the host and suggesting that iron acquisition is a key step in the establishment and development of this pathogen during

**Correspondence:** Dr. Maria Eugenia Rodriguez, CINDEFI, Facultad de Ciencias Exactas, Universidad Nacional de La Plata, calles 47 y 115, La Plata, Argentina

**E-mail:** mer@quimica.unlp.edu.ar

**Fax:** +54-221-48-33794

\*Both authors contributed equally to this work.

**Colour Online:** See the article online to view Figs. 1 and 3 in colour.

infection. The study of changes induced by iron starvation might then contribute to gain a deeper insight into the phenotype induced within the host, eventually leading to a better understanding of host–pathogen interaction.

Several of the high affinity systems through which *B. pertussis* can acquire iron have been already identified [5]. However, only a few studies aiming at dissecting the global adaptive response induced by iron starvation were reported so far. Early approaches assessed differences in protein profiles by mean of SDS-PAGE [6, 7]. These studies, however, did not include the identification of the proteins differentially expressed. In 2003, the complete genome of *B. pertussis* strain Tohama I was sequenced [8] which constituted the basis for “omics” studies. In 2007, we reported the first analysis of the *B. pertussis* Tohama I proteome and proteome alterations induced by iron starvation as performed by means of 2DE [9]. The spot excision and subsequent MALDI-TOF MS allowed the identification of several new proteins induced by iron starvation. Twenty-three proteins with different levels in response to low iron availability were detected, eight showing lower protein levels and 15 showing higher levels than those detected in bacteria grown under iron replete conditions [9]. A number of new proteins with increased abundance under physiological conditions were identified by that proteome analysis. Among them were two antigens that were later recognized as potential components of a new generation of pertussis vaccines [10, 11]. Recently, Brickman *et al.* [12] have profiled gene expression in *B. pertussis* grown under iron-replete and iron-depleted conditions creating a global picture of differential gene transcription. However, due to post-transcriptional or post-translational regulation, as well as protein degradation, this profile may not necessarily reflect the bacterial proteome.

The development of better techniques to separate peptides and proteins, together with the improvements in MS instrumentation and computational analysis tools allowed the analysis of complex protein samples by shotgun proteomics, a technique that combines protein digestion, nano-LC, and MS/MS-based peptide identification [13]. Shotgun and 2DE proteomics are techniques that provide complementary information [14]. In this study, we used sensitive shotgun proteomics to gain a deeper insight into the complex response of *B. pertussis* to iron availability.

## 2 Material and methods

### 2.1 Bacterial strain and growth conditions

*Bordetella pertussis* strain BP536, a streptomycin-resistant derivative of Tohama I was used in this study. For phagocytosis experiments, *B. pertussis* BP536 was transformed with plasmid pCW505 [15] (kindly supplied by Dr. Weiss, Cincinnati, OH, USA) which induces cytoplasmic expression of GFP without affecting growth or antigen expression [15]. *Bordetella pertussis* was cultured as previously described [9]. Briefly, bacteria were grown at 35°C on Bordet Gengou agar (BGA)

plates supplemented with 15% defibrinated sheep blood. After 3 days, bacteria were subcultured in Stainer-Scholte (SS) liquid medium and maintained under shaking conditions at 37°C for 24 h. Bacterial cells were harvested by centrifugation ( $10\,000 \times g$  for 15 min at room temperature), washed with sterile iron-free saline solution, and used to inoculate 100 mL of iron-replete SS (36  $\mu\text{M}$  iron) and iron-depleted SS (without addition of  $\text{FeSO}_4 \cdot 7\text{H}_2\text{O}$ ). Bacteria were further cultured at 37°C for 20 h, subcultured twice in the respective culture media, and grown until late exponential phase. Iron-depleted medium was prepared as described before [9]. Siderophores in culture supernatants of *B. pertussis* grown in iron-depleted medium were investigated by the chrome azurol S (CAS) assay [16] and used to confirm iron-limited growth. Three independent replicates were prepared for both iron-depleted and iron-replete conditions.

### 2.2 Identification of *B. pertussis* proteins by nano-LC-LTQ-Orbitrap-MS/MS

*Bordetella pertussis* grown either in iron-depleted (Bp-Fe) or iron-replete (Bp+Fe) SS medium were harvested and cell lysates were prepared. Briefly, cells from 10 mL of culture were collected by centrifugation at  $10\,000 \times g$  for 10 min at 4°C, washed twice with milliQ water, and resuspended in 50  $\mu\text{L}$  of urea/thiourea (8M/2M) (UT). Proteins were solubilized during 1 h at room temperature (RT) and centrifuged at  $20\,000 \times g$  at 20°C for 1 h. Total protein concentration in the supernatant was determined using a Bradford assay (Bio-rad, Munich, Germany). Finally, 4  $\mu\text{g}$  of proteins solubilized in UT were further diluted in 20 mM ammonium bicarbonate, reduced with 25 mM DTT (1 h, 60°C), alkylated with 100 mM iodoacetamide (30 min, 37°C), and proteolytically digested with 4  $\mu\text{L}$  of trypsin (0.25  $\mu\text{g}/\mu\text{L}$ ) (Promega, Madison, WI, USA) overnight in a water bath at 37°C [17]. The tryptic digestion was stopped by addition of trifluoroacetic acid (TFA) (Merck, Darmstadt, Germany) to a final concentration of 0.1% v/v. Cellular debris was removed by centrifugation at  $16\,000 \times g$  for 10 min at RT. The supernatant was transferred to a 1.5 mL tube and peptides were purified and desalted using C18-ZipTip columns (Merck Millipore, Billerica, MA, USA). A commercial vacuum centrifuge concentrator was used to remove acetonitrile. MS was performed on a Proxeon nano-LC system (Proxeon, Odense, Denmark) connected to an LTQ-Orbitrap-MS (ThermoElectron, Bremen, Germany) equipped with a nano-ESI source. For LC separation, an Acclaim PepMap100 column capillary of 15 cm bed length (C18, 3 mm, 100A) (Dionex, Sunnyvale CA, USA) was used. The flow rate used was 300 nL/min for the nano column and the solvent gradient ranged from 0% B (15 min) to 60% B (290 min). Solvent A was 0.1% acetic acid and 2% ACN, whereas 100% ACN with 0.1% acetic acid was used as solvent B. The MS was operated in data-dependent mode to automatically switch between Orbitrap-MS and LTQ-MS/MS acquisition.

Survey full-scan MS spectra ( $m/z$  300–2000) were acquired in the Orbitrap with a resolution  $R$  60000 at  $m/z$  400. The method used allowed sequential isolation of up to five of the most intense ions, depending on signal intensity, for fragmentation on the linear ion trap using CID at a target value of 10 000 ions. The dynamic exclusion time window was set to 60 s. General MS conditions were electrospray voltage, 1.5 kV; no sheath and auxiliary gas flow. Ion selection threshold was set to 500 MS counts for MS/MS selection. An activation  $Q$ -value of 0.25 and activation time of 30 ms were used.

The MS data have been deposited to the ProteomeXchange Consortium (<http://proteomecentral.proteomexchange.org>) via the PRIDE partner repository [18] with the dataset identifier PXD001280.

### 2.3 Analysis of MS data

For protein identification, the raw data were post-processed with the Sorcerer<sup>TM</sup> software package v3.5 (Sage-N Research Inc. Milpitas, CA, USA). After conversion, all tandem-MS spectra were searched using the SEQUEST<sup>®</sup> search engine (ThermoFinnigan, San Jose, CA, USA, version v.27, rev.11). SEQUEST<sup>®</sup> was set up to search against the *B. pertussis* Tohama I FASTA database (3761 entries for *B. pertussis* Tohama I, release 02/2012) assuming the digestion with trypsin. SEQUEST<sup>®</sup> searches were performed with a precursor ion tolerance of 20 ppm and a fragment ion mass tolerance of 1 Da. Oxidation of methionine was specified in SEQUEST<sup>®</sup> as variable modification. Peptide identifications were accepted if they exceeded specific database search engine thresholds. SEQUEST<sup>®</sup> identifications required at least deltaCn scores of greater than 0.10 and XCorr scores of greater than 2.2, 3.8, and 3.8 for doubly, triply, and quadruply charged peptides, respectively. Proteins that contained similar peptides and could not be differentiated based on tandem MS/MS analysis alone were grouped to satisfy the principles of parsimony. Scaffold software (Proteome Software, Portland, OR, USA) was used to validate protein identifications derived from MS/MS sequencing results. Scaffold verifies peptide identifications assigned by SEQUEST<sup>®</sup> using the X!Tandem database search program [19]. Peptide and protein identifications were accepted if they could be established at  $\geq 95\%$  probability respectively, as specified by the Peptide Prophet algorithm [20]. Protein probabilities were assigned by the Protein Prophet algorithm [21]. Protein identifications were accepted if they reached greater than 99% probability and contained at least two identified unique peptides. These identification criteria typically established  $<0.01\%$  false discovery rate (FDR) based on a decoy database search strategy at the protein level. Identified peptides/proteins were quantified using unweighted spectral counting. To this end, spectra identified for a specific protein in a dataset were normalized to the total spectra identified in that dataset and then a ratio of the relative quantities in the different conditions was calculated. This

normalization, which is performed by using a display option called “quantitative value” in Scaffold v3.0, was used to determine relative abundance of proteins within datasets [22]. The normalized data for each abundance ratio comparison was tested for significance using two-group t-test for each condition. The  $p$ -values were further adjusted for multiple testing to control the FDR at a cut-off of 0.05 following the Benjamini–Hochberg procedure [23]. The two-group t-test and multiple testing corrections were performed using the Genedata Analyst v8.2 software (Genedata AG, Basel, Switzerland). Proteins showing a Benjamini–Hochberg  $q$ -value of 0.05 or less were regarded as significantly regulated. Eventually, proteins that showed a  $q$ -value higher than 0.05 but lower than 0.1 were included with the purpose of interpreting the overall trend of a selected dataset. In those cases, the  $q$ -value was expressed between brackets. Biological relevance threshold was set when an absolute fold change of 1.5 was exceeded.

The proteins were further functionally classified as assigned by the descriptive multifunctional classification of Serres and Riley [24], in the categories “metabolism” (MultiFun category 1), “information transfer” (MultiFun category 2), “regulation” (MultiFun category 3), “transport” (MultiFun category 4), “cell processes” (MultiFun category 5), and “cell structure” (MultiFun category 6). A total of 677 proteins were classified based on MultiFun categories. Those proteins with a putative function that has only been assigned by homology to other proteins, without biological evidence, were included in the MultiFun classification, according to their respective predicted function. The other 249 proteins were further included two other categories, namely, “virulence factors” (known *B. pertussis* virulence factors) and “hypothetical and conserved hypothetical” (no *Escherichia coli* homolog or unknown molecular function).

### 2.4 Cells

Peripheral blood neutrophils (PMN) were isolated from heparinized venous blood using Ficoll-Histopaque (Sigma, St. Louis, MO, USA) gradient centrifugation. Briefly, PMN were harvested and treated with hypotonic solution to remove remaining erythrocytes. PMN purity exceeded 95%. Cell viability, as determined by trypan blue exclusion, was 99%. PMN were washed twice with DMEM supplemented with 0.2% of BSA (Sigma), suspended, and used immediately. All experiments described in this study were carried out with PMN lacking Fc $\gamma$ RI (CD64) expression, as monitored by FACS analysis with anti-Fc $\gamma$ RI mAb 22 (BD Biosciences, San Diego, CA, USA).

### 2.5 Antibodies

The 4–37F3 (IgG1) against *B. pertussis* FHA monoclonal antibody [25], kindly provided by the Netherlands Vaccine Institute, Bilthoven, the Netherlands, was used in this study.

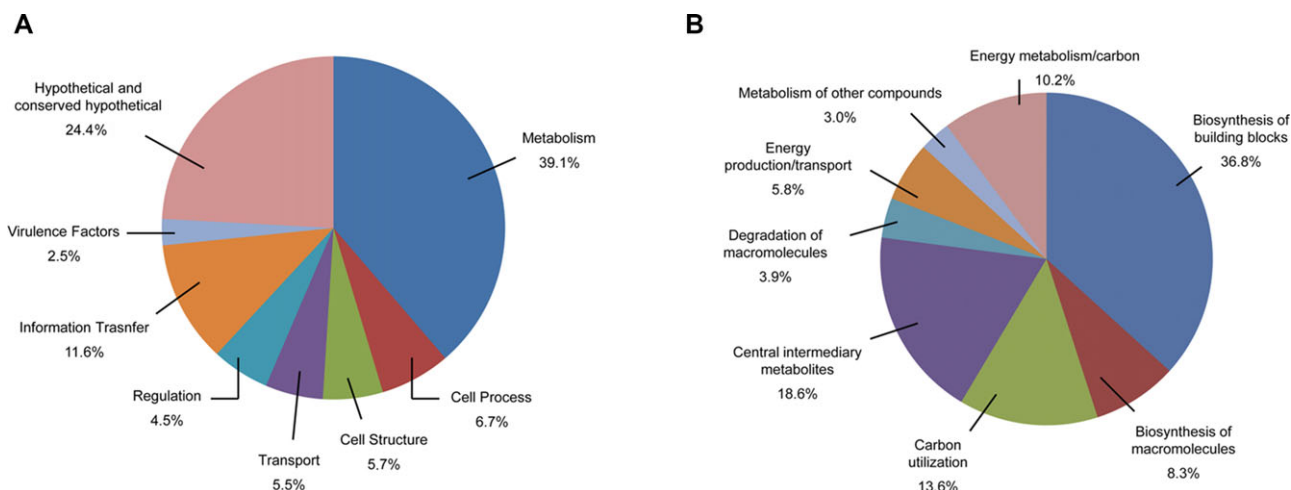


**Figure 1.** Classification of the identified *Bordetella pertussis* proteins into functional categories (A) Classification of the identified proteins according to their cellular function. (B) Proteins belonging to the category “metabolism” classified according to their known or predicted function.

Polyclonal mouse anti-CyaA *B. pertussis* antiserum was generated as described before [26].

## 2.6 Phagocytosis assay

Phagocytosis of *B. pertussis* was evaluated by confocal microscopy as previously described [27] with a few modifications. GFP-expressing Bp-Fe or Bp+Fe were incubated with PMN for 10 min at 37°C to allow interaction (multiplicity of infection (MOI): 200), extensively washed at 4°C to remove nonattached bacteria and further incubated for 40 min at 37°C. Phagocytosis was stopped by placing PMN on ice. Cells were then fixed using 4% paraformaldehyde, washed once with PBS, and incubated for 10 min at RT with PBS containing 50 mM NH<sub>4</sub>Cl. PMN surface-bound bacteria were detected by a two-step antibody-dependent labeling procedure as follows. PMN were incubated with polyclonal rabbit anti-*B. pertussis* antiserum (30 min at 4°C), followed by incubation with CY3-conjugated goat F(ab')<sub>2</sub> fragments of antirabbit immunoglobulin for another 30 min at 4°C. After two washing steps, the cells were permeabilized by incubation with PBS containing 0.1% saponin (Sigma-Aldrich) and 0.2% BSA for 30 min, and further incubated for other 30 min with rabbit anti-*B. pertussis* antiserum in the presence of 0.1% saponin and 0.2% BSA in order to determine the number of intracellular bacteria. After washing three times, PMN were incubated for 30 min with FITC-conjugated F(ab')<sub>2</sub> of goat anti-rabbit IgG1. Labeling of the bacteria with FITC-conjugated antibodies was performed to minimize the loss of read-out sensitivity due to quenching of GFP fluorescence after internalization. Finally, cells were spun on microscope slides. Microscopic analyses were performed using a confocal laser scanning microscope (Leica TCS SP5, Germany). The number of extra-

cellular (red and green fluorescent) and intracellular bacteria (green fluorescent) per cell was determined by microscopic examination of 20 randomly selected fields showing a minimum of five cells per field.

Differences between the mean values of the phagocytosis experiments were evaluated by mean of ANOVA. Significance was accepted at  $p < 0.05$ . Results are shown as means and standard deviation (SD).

## 2.7 Western blot analysis

Ten micrograms of crude bacterial protein extract of *B. pertussis* grown in the presence (Bp+Fe) or absence (Bp-Fe) of iron were resolved by 7.5% SDS-PAGE. Proteins were transferred to polyvinylidene difluoride (Immobilon PVDF Millipore) sheets [28] and incubated with mouse anti-FHA (1:500) or mouse anti-CyaA (1:500) antibodies. HRP-conjugated goat antimouse IgG antibodies (Jackson ImmunoResearch, Baltimore Pike, 1:2500) were used for immunochemical detection. An ECL Western Blotting Detection Reagent (Pierce Biotechnology, Rockford, IL, USA) was used to detect specific signals.

## 3 Results and discussion

In this study, the proteome profile of *B. pertussis* grown under either low iron availability or iron-replete conditions was analyzed and compared. This analysis provided a final list of 926 identified proteins (Supplemental Material, Supporting Information Table 1) which represent 24% of all *B. pertussis* coding sequences [8]. The functional classification of identified proteins showed that most of them belong to the categories “metabolism” (39%), “hypothetical and conserved hypothetical” (20%), or “information transfer” (14%) (Fig. 1A). The

category “metabolism” was further divided into eight sub-categories (Fig. 1B). This more specific analysis showed that most of the identified proteins are involved in biosynthesis of building blocks such as amino acids, cofactors, and nucleotides.

The comparison of the protein patterns of iron-starved and iron-replete bacteria revealed 98 proteins displaying differential levels (Supplemental Material, Supporting Information Table 2, sheet 1 and sheet 2), which represent 10.5% of the total proteins identified by the proteome analysis, suggesting that iron starvation provoked a remarkable shift in protein composition. The highest percentage of iron-regulated proteins was found within the “virulence factors” category, with 32% of the proteins exhibiting a lower abundance under iron starvation. Interestingly, none of the proteins belonging to this category showed higher abundance in response to iron starvation. Among the other categories, 19% of the proteins involved in bacterial adaptation (“cell processes” category), 10% of the proteins belonging to “metabolism”, and 6.25% of the proteins included in “information transfer” were influenced in level by iron availability.

### 3.1 Adaptation and protection proteins

Several proteins included in the “adaptation/protection” category showed increased abundance in iron-starved *B. pertussis* (Supplemental Material, Supporting Information Table 2, sheet 1). Most of them are involved in iron acquisition, including BhuT (BP0345), BhuS (BP0346), and BhuR (BP0347), required for the uptake and utilization of heme [3], and AlcC (BP2458), involved in alcaligin biosynthesis [29]. The level of the putative siderophore receptors BfrB (BP2016) and BfrI (BP1962), previously found with elevated amounts under these environmental conditions by 2DE proteomics [9], was also observed as increased. Additionally, although their differential levels were not statistically significant, two proteins, BhuV (BP0343,  $q = 0.053$ ) belonging to *Bordetella* heme utilization (*bhu RSTUV*) and AlcB (BP2457,  $q = 0.069$ ) belonging to alcaligin biosynthesis (*alc ABCDER*), were also found increased under iron starvation. The same was observed for the alcaligin receptor FauA (BP2463,  $q = 0.077$ ). ArgC (BP2960), a protein not directly involved in iron acquisition but implicated in ornithine biosynthesis, an alcaligin amino acid precursor [30], also showed increased levels under iron starvation. Finally, IRP1-3 (BP1152), an iron-regulated protein already identified by 2DE proteomics [9], was also found in higher amounts under iron starvation in this study. This protein is presumed to play a role during infection [31] and was found to be a good vaccine candidate [10, 11].

Oxidative stress and iron metabolism are often related. Iron reacts with hydrogen peroxide to generate hydroxyl radicals [32] which are highly reactive and extremely harmful. The increased expression of iron acquisition systems might lead to a transient increase in the intracellular iron level despite the low extracellular concentration, eventually determining a higher level of reactive oxygen intermediates. In this study,

we found iron starvation to increase the abundance of SodA (BP0193), a Mn<sup>2+</sup>-containing superoxide dismutase [33] (Supplemental Material, Supporting Information Table 2, sheet 1). Also AhpC (BP3552,  $q = 0.059$ ), an alkyl hydroperoxide reductase, involved in the bacterial defence against oxidative stress, and AhpD (BP3551,  $q = 0.079$ ), a protein predicted to be required for the reduction of the cysteine residues of the active site of AhpC, were found at increased levels in iron-starved *B. pertussis*. Although the  $q$ -values of AhpC and AhpD were higher than the threshold set in our statistical analysis, the observed increase in the abundance of both proteins under iron limitation is likely to be of significance since they are proteins that are known to be induced under these environmental conditions, as found in *Campylobacter jejuni* [34], *Corynebacterium diphtheriae* [35], and *Bacillus subtilis* [36, 37].

These results suggest that iron starvation simultaneously induced a bacterial adaptation to potentially higher levels of reactive oxygen species during infection.

### 3.2 Information transfer and metabolism

We observed lower levels of NrdA (BP2983), a protein involved in DNA replication, and of two proteins involved in DNA transcription, RpoC (BP0016) and RpoB (BP0015) during iron starvation. The same was observed for three proteins involved in translation, two ribosomal proteins (BP2793 and BP3618) and glutamyl-tRNA synthetase (BP3226) (Supplemental Material, Supporting Information Table 2, sheet 2). Whereas these results might initially suggest a general shutdown of metabolic processes, a closer look at the category “metabolism” showed that the level of many proteins involved in carbon utilization, energy metabolism, and central intermediary metabolism, was increased under iron starvation (Supplemental Material, Supporting Information Table 2, sheet 1). This increase is probably linked to house-keeping functions and bacterial viability. We also observed changes in the protein levels of different known and putative ABC transporters for amino acids. From our results, however, no clear conclusions on amino acid-scavenging mechanisms favored by iron starvation could be drawn.

Fatty acid degradation and nutrient starvation were previously found connected [38, 39]. Stringent response of *E. coli* comprises the upregulation of several genes involved in fatty acid degradation [40]. In the present study, we observed a similar response in *B. pertussis*. The abundance of BP0624, BP0625, and BP2377, proteins involved in fatty acid utilization, was found increased under iron starvation (Supplemental Material, Supporting Information Table 2, sheet 1). BP0624 is an acyl-CoA synthase that activates fatty acids by binding them to coenzyme A, the first step of fatty acid degradation. BP2377 is a putative AMP-binding protein similar to many predicted fatty-acid-CoA ligases. BP0625 is a probable acyl-CoA dehydrogenase involved in fatty acid degradation. Through  $\beta$ -oxidation, fatty acids are completely degraded to acetyl-CoA, which might

eventually be converted to acetoacetyl-CoA. The level of the acetoacetyl-CoA reductase (BP1150) was also found increased in iron-starved bacteria (Supplemental Material, Supporting Information Table 2, sheet 1). This protein catalyses the conversion of acetoacetyl-CoA into (R)-3-hydroxybutanoyl-CoA, a precursor of the poly-hydroxybutyrate (PHB), which serves as a storage polymer. Another source of acetyl-CoA is pyruvate. *Bordetella pertussis* produces acetyl-CoA from pyruvate through a pathway catalyzed by the pyruvate dehydrogenase complex. The levels of  $\alpha$  and  $\beta$  subunits of the putative pyruvate dehydrogenase E1 (BP0629 and BP0628, respectively), dihydrolipoamide acetyltransferase (BP0994), and dihydrolipoamide dehydrogenase (BP0995), all of them components of the pyruvate dehydrogenase complex, were found increased under iron starvation (Supplemental Material, Supporting Information Table 2, sheet 1). Two other proteins involved in butanoate metabolism, BP0627 and BP0217 (Supplemental Material, Supporting Information Table 2, sheet 1) showed higher abundance in iron-starved bacteria. BP0627 is a probable enoyl-CoA hydratase/isomerase that catalyzes the conversion of crotonoyl-CoA, an intermediary in butanoate degradation, into (S)-3-hydroxybutanoyl-CoA. This molecule is converted into acetoacetyl-CoA by a reaction catalyzed by the 3-hydroxybutyryl-CoA dehydrogenase (BP0217), a protein that was found twofold increased in iron-starved *B. pertussis*.

Altogether, these results suggest that under iron starvation, *B. pertussis* stores energy and carbon in the form of PHB (Supplemental Material, Supporting Information Fig. 1), a storage polymer that can be rerouted into the main metabolism, an observation that has been made before for *B. pertussis* growing under a stoichiometric excess of carbon and energy sources [41].

### 3.3 Virulence factors

In the present study, the levels of most of the virulence factors regulated by the BvgAS system were found decreased under iron starvation (Supplemental Material, Supporting Information Table 2, sheet 2). Among them were adhesins, such as filamentous hemagglutinin (FHA, BP1879) [42, 43] and fimbriae (Fim, BP1119) [44], and the target of opsonic antibodies, pertactin (Prn, BP1054) [45] (Supplemental Material, Supporting Information Table 2, sheet 2). The level of bacterial toxin adenylate cyclase (CyaA, BP0760) was also found decreased in iron-starved bacteria (Supplemental Material, Supporting Information Table 2, sheet 2). Similarly, two components of the type IV secretion system required for pertussis toxin secretion through the outer membrane, PtlE (BP3793) and PtlF (BP3794), were found in decreased amounts (PtlF) or were even absent (PtlE) in the proteome of iron-starved *B. pertussis* (Supplemental Material, Supporting Information Table 2, sheet 2, “transport” category). The levels of three other virulence factors, the autotransporters TcfA (BP1201), BrkA (BP3494), and Vag8 (BP2315), were decreased by iron



**Figure 2.** Western blot analysis of *Bordetella pertussis* virulence factors. Crude protein extracts of *B. pertussis* grown in the presence (Bp+Fe) or the absence (Bp-Fe) of iron were run in SDS-PAGE (7.5%) and transferred to PVDF membranes. Immunoblot analysis was performed with mouse antibodies raised against (A) FHA, or (B) CyaA. The gels were loaded with the same amount of proteins of each sample. For reference, the position of the molecular weight marker 205 kDa is indicated in each panel.

starvation (Supplemental Material, Supporting Information Table 2, sheet 2).

The differential abundance of the main virulence factors was further analyzed by Western blot analysis. The decrease in the abundance of FHA and CyaA in iron-starved bacteria was clearly confirmed by this technique (Fig. 2).

The production of all the proteins mentioned above is positively controlled by the BvgAS two-component signal transduction system in response to environmental conditions [46, 47]. This system is activated when the bacteria grow at 37°C and inactivated at 25°C or in the presence of modulators like nicotinic acid or MgSO<sub>4</sub> [48]. In the present study, we showed that iron starvation triggers a decrease in the level of most of the virulence factors regulated by the BvgAS system despite the absence of the so-called modulating conditions during growth. Previous transcriptomic studies reported that low iron availability induces an increase in the transcript abundance of some of the BvgAS regulated genes in *B. pertussis* [12]. This discrepancy between transcriptome and proteome data might be due to post-transcriptional or post-translational regulation either influencing protein synthesis or stability. Recently, Bibova *et al.* showed that Hfq, a small RNA chaperone, is involved in post-transcriptional regulation of *B. pertussis* virulence [49] suggesting a role for sRNA in this process. The involvement of small RNA (either dependent or independent of Hfq) in the iron-induced modulation of virulence might explain the discrepancy between transcriptomic and proteomic data, an observation that deserves further investigation.

Given that most of the bacterial virulence factors mentioned above are implicated in host infection, the lower levels of these proteins under physiological conditions might play a role in this process. *Bordetella pertussis* infection is initiated by the attachment of this pathogen to the upper respiratory tract epithelial cells. The lower level of adhesins under iron starvation might lead to a lower attachment of *B. pertussis* to host cells. However, we previously showed that this pathogen increases its attachment capacity to respiratory epithelial cells in the absence of iron in a FHA-independent manner [50]. Once the mucosal surface of the respiratory tract has been colonized by the bacteria, the local immune response recruits immune cells. The adhesin FHA is also involved in the innate interaction of *B. pertussis* with host immune cells

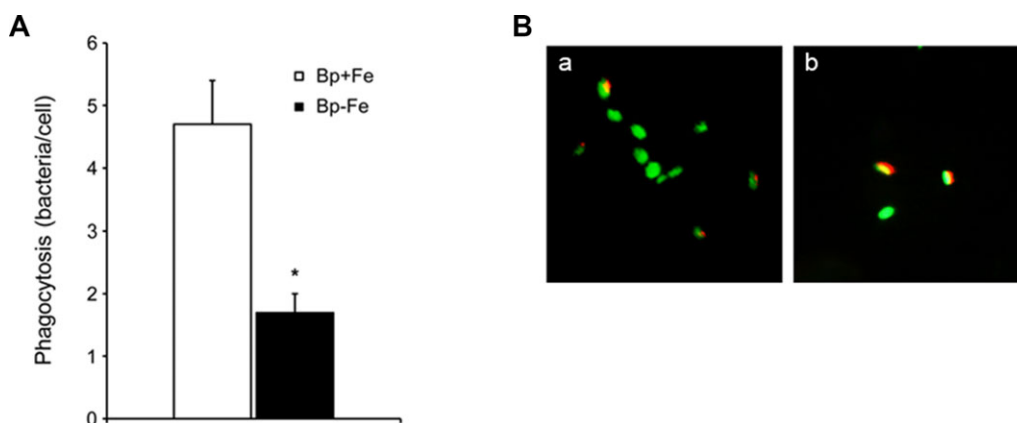


**Figure 3.** *Bordetella pertussis* phagocytosis by PMN. (A) *Bordetella pertussis* grown in the presence (Bp+Fe) or the absence (Bp-Fe) of iron were incubated with PMN (MOI of 200) for 10 min at 37°C. After attachment, PMN were washed and further incubated for 40 min at 37°C to allow internalization. Cells were fixed, intracellular bacteria were labeled with green fluorescent dye and extracellular bacteria with both green and red fluorescent dyes. Bacterial phagocytosis was assessed by confocal laser scan fluorescence microscopy. To assess the number of phagocytosed bacteria at least 100 cells were counted per slide. The data represent the mean  $\pm$  SD of four experiments with PMN from different donors. Phagocytosis of Bp-Fe by PMN differed significantly ( $*p < 0.05$ ) from PMN phagocytosis of Bp+Fe. (B) Confocal fluorescence microscopy of PMN incubated 40 min at 37°C with *B. pertussis* grown in the presence (a) or the absence (b) of iron. Representative panels of one out of four independent experiments are shown.

eventually leading to a CR3-mediated bacterial phagocytosis [51, 52]. Thus, the decrease in the level of FHA observed during iron starvation might decrease the recognition of bacteria by these cells without affecting the interaction with epithelial cells. In order to examine the interaction of iron-starved *B. pertussis* with host immune cells, we analyzed the bacterial uptake by PMN. To this end, bacteria grown either under iron-replete or iron-depleted conditions were incubated with PMN for 40 min. The number of *B. pertussis* phagocytosed by PMN was evaluated by double fluorescence microscopy. Iron starvation significantly decreased the number of bacteria attached to and phagocytosed by PMN (Fig. 3) suggesting that physiological conditions might eventually increase the odds of bacterial survival upon the encounter with immune cells.

#### 4 Concluding remarks

*Bordetella pertussis* responds to the lack of free iron by changing the levels of a rather large number of proteins involved in a wide range of bacterial functions. As expected, the levels of proteins related to iron acquisition were found significantly increased. Bacterial metabolism seems to be redirected to maintain house-keeping functions and to form PHB which might be metabolized when external carbon sources become less available. Iron starvation was further observed to induce a significant decrease in the cellular level of most of the virulence factors regulated by the BvgAS system, eventually shaping host–pathogen interaction. How iron starvation affects *B. pertussis* interaction with respiratory cells was already shown in previous studies [50], while the influence on bacterial interaction with immune cells was shown in this article. Both results support the assumption that bacterial

adaptation to iron starvation induces phenotypic changes that facilitate host colonization. Proteins potentially related to oxidative stress resistance were produced in higher amounts in response to low iron availability, which might further improve the adaptation to host defense mechanisms. Taken together, these findings open new possibilities to better understand the role of iron in the pathogenesis of *B. pertussis*. Further investigations on transcriptional and post-transcriptional processes controlling the adaptation of this pathogen to low iron availability, should be considered.

*This study was partially supported by the ANPCyT (PICT 0413 and PICT 2131) CONICET (Res. N 2622), and DAAD and the BMBF/“Unternehmen Region” as part of the ZIK-FunGene. M.E.R., J.A.H., and Y.L. are members of the Scientific Career of CONICET.*

*The authors have declared no conflict of interest.*

#### 5 References

- [1] Moore, C. H., Foster, L. A., Gerbig, D. G., Jr., Dyer, D. W., Gibson, B. W., Identification of alcaligin as the siderophore produced by *Bordetella pertussis* and *B. bronchiseptica*. *J. Bacteriol.* 1995, 177, 1116–1118.
- [2] Beall, B., Sanden, G. N., A *Bordetella pertussis* *fepA* homologue required for utilization of exogenous ferric enterobactin. *Microbiology* 1995, 141, 3193–3205.
- [3] Vanderpool, C. K., Armstrong, S. K., The *Bordetella* *bhu* locus is required for heme iron utilization. *J. Bacteriol.* 2001, 183, 4278–4287.
- [4] Brickman, T. J., Hanawa, T., Anderson, M. T., Suhadolc, R. J., Armstrong, S. K., Differential expression of *Bordetella*

- pertussis iron transport system genes during infection. *Mol Microbiol.* 2008, *70*, 3–14.
- [5] Brickman, T. J., Anderson, M. T., Armstrong, S. K., Bordetella iron transport and virulence. *Biometals* 2007, *20*, 303–322.
- [6] Redhead, K., Hill, T., Chart, H., Interaction of lactoferrin and transferrins with the outer membrane of *Bordetella pertussis*. *J. Gen. Microbiol.* 1987, *133*, 891–898.
- [7] Menozzi, F. D., Gantiez, C., Loch, C., Identification and purification of transferrin- and lactoferrin-binding proteins of *Bordetella pertussis* and *Bordetella bronchiseptica*. *Infect. Immun.* 1991, *59*, 3982–3988.
- [8] Parkhill, J., Sebahia, M., Preston, A., Murphy, L. D. et al., Comparative analysis of the genome sequences of *Bordetella pertussis*, *Bordetella parapertussis* and *Bordetella bronchiseptica*. *Nat. Genet.* 2003, *35*, 32–40.
- [9] Vidakovics, M. L., Paba, J., Lamberti, Y., Ricart, C. A. et al., Profiling the *Bordetella pertussis* proteome during iron starvation. *J. Proteome Res.* 2007, *6*, 2518–2528.
- [10] Alvarez Hayes, J., Erben, E., Lamberti, Y., Ayala, M. et al., Identification of a new protective antigen of *Bordetella pertussis*. *Vaccine* 2011, *29*, 8731–8739.
- [11] Alvarez Hayes, J., Erben, E., Lamberti, Y., Principi, G. et al., *Bordetella pertussis* iron regulated proteins as potential vaccine components. *Vaccine* 2013, *31*, 00687–00687.
- [12] Brickman, T. J., Cummings, C. A., Liew, S. Y., Relman, D. A., Armstrong, S. K., Transcriptional profiling of the iron starvation response in *Bordetella pertussis* provides new insights into siderophore utilization and virulence gene expression. *J. Bacteriol.* 2011, *193*, 4798–4812.
- [13] Link, A. J., Eng, J., Schieltz, D. M., Carmack, E. et al., Direct analysis of protein complexes using mass spectrometry. *Nat. Biotechnol.* 1999, *17*, 676–682.
- [14] Schmidt, F., Donahoe, S., Hagens, K., Mattow, J. et al., Complementary analysis of the *Mycobacterium tuberculosis* proteome by two-dimensional electrophoresis and isotope-coded affinity tag technology. *Mol. Cell. Proteomics.* 2004, *3*, 24–42.
- [15] Weingart, C. L., Broitman-Maduro, G., Dean, G., Newman, S. et al., Fluorescent labels influence phagocytosis of *Bordetella pertussis* by human neutrophils. *Infect. Immun.* 1999, *67*, 4264–4267.
- [16] Schwyn, B., Neilands, J. B., Universal chemical assay for the detection and determination of siderophores. *Anal. Biochem.* 1987, *160*, 47–56.
- [17] Schmidt, F., Scharf, S. S., Hildebrandt, P., Burian, M. et al., Time-resolved quantitative proteome profiling of host-pathogen interactions: the response of *Staphylococcus aureus* RN1HG to internalisation by human airway epithelial cells. *Proteomics* 2010, *10*, 2801–2811.
- [18] Vizcaino, J. A., Deutsch, E. W., Wang, R., Csordas, A. et al., ProteomeXchange provides globally coordinated proteomics data submission and dissemination. *Nat. Biotechnol.* 2014, *32*, 223–226.
- [19] Craig, R., Beavis, R. C., A method for reducing the time required to match protein sequences with tandem mass spectra. *Rapid Commun. Mass Spectrom.* 2003, *17*, 2310–2316.
- [20] Keller, A., Nesvizhskii, A. I., Kolker, E., Aebersold, R., Empirical statistical model to estimate the accuracy of peptide identifications made by MS/MS and database search. *Anal. Chem.* 2002, *74*, 5383–5392.
- [21] Nesvizhskii, A. I., Keller, A., Kolker, E., Aebersold, R., A statistical model for identifying proteins by tandem mass spectrometry. *Anal. Chem.* 2003, *75*, 4646–4658.
- [22] Lundgren, D. H., Hwang, S. I., Wu, L., Han, D. K., Role of spectral counting in quantitative proteomics. *Expert Rev. Proteomics* 2010, *7*, 39–53.
- [23] Benjamini, Y., Drai, D., Elmer, G., Kafkafi, N., Golani, I., Controlling the false discovery rate in behavior genetics research. *Behav. Brain Res.* 2001, *125*, 279–284.
- [24] Serres, M. H., Riley, M., MultiFun, a multifunctional classification scheme for *Escherichia coli* K-12 gene products. *Microb. Comp. Genomics* 2000, *5*, 205–222.
- [25] Poolman, J. T., Kuipers, B., Vogel, M. L., Hamstra, H. J., Nagel, J., Description of a hybridoma bank towards *Bordetella pertussis* toxin and surface antigens. *Microb. Pathog.* 1990, *8*, 377–382.
- [26] Hozbor, D., Chirido, F. G., Rodriguez, M. E., Valverde, C., Yantorno, O., Quantitation of adenylate cyclase of *Bordetella pertussis* by enzyme linked immunosorbent assay. *Biologicals.* 1995, *23*, 279–284.
- [27] Gorgojo, J., Lamberti, Y., Valdez, H., Harvill, E. T., Rodriguez, M. E., *Bordetella parapertussis* survives the innate interaction with human neutrophils by impairing bactericidal trafficking inside the cell through a lipid raft-dependent mechanism mediated by the lipopolysaccharide O antigen. *Infect. Immun.* 2012.
- [28] Towbin, H., Staehelin, T., Gordon, J., Electrophoretic transfer of proteins from polyacrylamide gels to nitrocellulose sheets: procedure and some applications. *Proc. Natl. Acad. Sci. USA* 1979, *76*, 4350–4354.
- [29] Kang, H. Y., Brickman, T. J., Beaumont, F. C., Armstrong, S. K., Identification and characterization of iron-regulated *Bordetella pertussis* alcaligin siderophore biosynthesis genes. *J. Bacteriol.* 1996, *178*, 4877–4884.
- [30] Brickman, T. J., Armstrong, S. K., The ornithine decarboxylase gene *odc* is required for alcaligin siderophore biosynthesis in *Bordetella* spp.: putrescine is a precursor of alcaligin. *J. Bacteriol.* 1996, *178*, 54–60.
- [31] Brickman, T. J., Armstrong, S. K., Iron and pH-responsive FtrABCD ferrous iron utilization system of *Bordetella* species. *Mol. Microbiol.* 2012, *86*, 580–593.
- [32] Andrews, S. C., Robinson, A. K., Rodriguez-Quinones, F., Bacterial iron homeostasis. *FEMS Microbiol. Rev.* 2003, *27*, 215–237.
- [33] Graeff-Wohlleben, H., Killat, S., Banemann, A., Guiso, N., Gross, R., Cloning and characterization of an Mn-containing superoxide dismutase (SodA) of *Bordetella pertussis*. *J. Bacteriol.* 1997, *179*, 2194–2201.



- [34] Baillon, M. L., vanVliet, A. H., Ketley, J. M., Constantinidou, C., Penn, C. W., An iron-regulated alkyl hydroperoxide reductase (AhpC) confers aerotolerance and oxidative stress resistance to the microaerophilic pathogen *Campylobacter jejuni*. *J. Bacteriol.* 1999, *181*, 4798–4804.
- [35] Tai, S. S., Zhu, Y. Y., Cloning of a *Corynebacterium diphtheriae* iron-repressible gene that shares sequence homology with the AhpC subunit of alkyl hydroperoxide reductase of *Salmonella typhimurium*. *J. Bacteriol.* 1995, *177*, 3512–3517.
- [36] Bsat, N., Chen, L., Helmann, J. D., Mutation of the *Bacillus subtilis* alkyl hydroperoxide reductase (ahpCF) operon reveals compensatory interactions among hydrogen peroxide stress genes. *J. Bacteriol.* 1996, *178*, 6579–6586.
- [37] Chen, L., Keramati, L., Helmann, J. D., Coordinate regulation of *Bacillus subtilis* peroxide stress genes by hydrogen peroxide and metal ions. *Proc. Natl. Acad. Sci. USA* 1995, *92*, 8190–8194.
- [38] Al Dahouk, S., Jubier-Maurin, V., Neubauer, H., Kohler, S., Quantitative analysis of the *Brucella suis* proteome reveals metabolic adaptation to long-term nutrient starvation. *BMC Microbiol.* 2013, *13*, 199.
- [39] Dong, T., Schellhorn, H. E., Global effect of RpoS on gene expression in pathogenic *Escherichia coli* O157:H7 strain EDL933. *BMC Genomics* 2009, *10*, 349.
- [40] Traxler, M. F., Summers, S. M., Nguyen, H. T., Zacharia, V. M. et al., The global, ppGpp-mediated stringent response to amino acid starvation in *Escherichia coli*. *Mol. Microbiol.* 2008, *68*, 1128–1148. Epub 02008 Apr 06222.
- [41] Thalen, M., vanden, I. J., Jiskoot, W., Zomer, B. et al., Rational medium design for *Bordetella pertussis*: basic metabolism. *J. Biotechnol.* 1999, *75*, 147–159.
- [42] Ishibashi, Y., Nishikawa, A., *Bordetella pertussis* infection of human respiratory epithelial cells up-regulates intercellular adhesion molecule-1 expression: role of filamentous hemagglutinin and pertussis toxin. *Microb. Pathog.* 2002, *33*, 115–125.
- [43] Ishibashi, Y., Relman, D. A., Nishikawa, A., Invasion of human respiratory epithelial cells by *Bordetella pertussis*: possible role for a filamentous hemagglutinin Arg-Gly-Asp sequence and alpha5beta1 integrin. *Microb. Pathog.* 2001, *30*, 279–288.
- [44] Mooi, F. R., Jansen, W. H., Brunings, H., Gielen, H. et al., Construction and analysis of *Bordetella pertussis* mutants defective in the production of fimbriae. *Microb. Pathog.* 1992, *12*, 127–135.
- [45] Hellwig, S. M., Rodriguez, M. E., Berbers, G. A., vande Winkel, J. G., Mooi, F. R., Crucial role of antibodies to pertactin in *Bordetella pertussis* immunity. *J. Infect. Dis.* 2003, *188*, 738–742. Epub 2003 Aug 2005.
- [46] Uhl, M. A., Miller, J. F., Autophosphorylation and phosphotransfer in the *Bordetella pertussis* BvgAS signal transduction cascade. *Proc. Natl. Acad. Sci. USA* 1994, *91*, 1163–1167.
- [47] Weiss, A. A., Hewlett, E. L., Myers, G. A., Falkow, S., Tn5-induced mutations affecting virulence factors of *Bordetella pertussis*. *Infect. Immun.* 1983, *42*, 33–41.
- [48] Melton, A. R., Weiss, A. A., Environmental regulation of expression of virulence determinants in *Bordetella pertussis*. *J. Bacteriol.* 1989, *171*, 6206–6212.
- [49] Bibova, I., Skopova, K., Masin, J., Cerny, O. et al., The RNA chaperone Hfq is required for virulence of *Bordetella pertussis*. *Infect. Immun.* 2013, *26*, 26.
- [50] Vidakovics, M. L., Lamberti, Y., Serra, D., Berbers, G. A. et al., Iron stress increases *Bordetella pertussis* mucin-binding capacity and attachment to respiratory epithelial cells. *FEMS Immunol. Med. Microbiol.* 2007, *51*, 414–421. Epub 2007 Aug 2029.
- [51] Relman, D., Tuomanen, E., Falkow, S., Golenbock, D. T. et al., Recognition of a bacterial adhesion by an integrin: macrophage CR3 (alpha M beta 2, CD11b/CD18) binds filamentous hemagglutinin of *Bordetella pertussis*. *Cell* 1990, *61*, 1375–1382.
- [52] Ishibashi, Y., Claus, S., Relman, D. A., *Bordetella pertussis* filamentous hemagglutinin interacts with a leukocyte signal transduction complex and stimulates bacterial adherence to monocyte CR3 (CD11b/CD18). *J. Exp. Med.* 1994, *180*, 1225–1233.